ACS Biomaterials SCIENCE & ENGINEERING

Article

pubs.acs.org/journal/abseba

Melting Away Pain: Decay of Thermal Nociceptor Transduction during Heat-Induced Irreversible Desensitization of Ion Channels

Min Lin,*[†,‡] Shao Bao Liu,[‡] Guy M. Genin,[§] YongJin Zhu,[‡] Meng Shi,[‡] Changchun Ji,[†,‡,∥] Ang Li,[⊥] Tian Jian Lu,[‡] and Feng Xu*[†,‡]

[†]The Key Laboratory of Biomedical Information Engineering of Ministry of Education, School of Life Science and Technology, [‡]Bioinspired Engineering and Biomechanics Center, and [⊥]Key Laboratory of Shaanxi Province for Craniofacial Precision Medicine Research, College of Stomatology, Xi'an Jiaotong University, Xi'an 710049, PR China

[§]Department of Neurological Surgery, Washington University School of Medicine, NSF Science and Technology Center for Engineering Mechanobiology, and School of Engineering, Washington University, St. Louis, Missouri 63110, United States

[∥]Department of Acupuncture, Shaanxi Hospital of Traditional Chinese Medicine, Xi'an 710003, PR China

Supporting Information

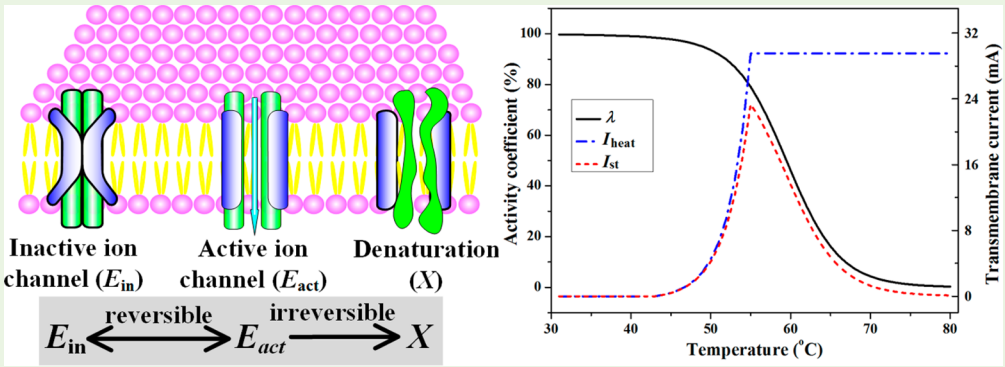

ABSTRACT: Thermal transient receptor potential channels play a key role in thermal sensation. Although predictive models exist for temperature-dependent transduction through these channels and for the associated sensations of pain, the ability to predict irreversible desensitization has been lacking. We explored the role of irreversible ion channel desensitization in pain sensation and hypothesized that desensitization of ion channels would follow the kinetics similar to the denaturation of catalytic enzymes. We therefore proposed a three-state model to simulate the kinetic of temperature-sensitive ion channels from the closed state through opening and irreversible thermal desensitization. We tested the model against data obtained in vivo from a feline model. The theoretical model predicts all experimental data with reasonable accuracy, and represents an important step toward the ability for understanding of the molecular basis of nociceptor signaling providing the possibility to design local anesthesia regimens and to the prediction of postoperative pain.

KEYWORDS: *Temperature-sensitive ion channels, Irreversible desensitization, Thermal pain, Trans-membrane ion transport*

1. INTRODUCTION

Pain is a significant health problem that affects the lives of millions of people worldwide and induces huge societal costs.[1,2] Pain resulting from heat is an important factor in a great number of therapies ranging from thermal ablation of soft tissues[3] to mandibular and dental sawing and drilling.[4,5] In all such therapies, anesthesia is desirable for controlling the transient pain that occurs between noxious heating and the ultimate desensitization of the temperature-gated ion channels whose openings can begin the cascade of thermal pain sensation.[6] These ion channels reside on the ends of the long axons of neurons called nociceptors that transduce noxious stimuli and mediate the selective passage of specific ions across the cell membrane at noxious temperature levels.[7−9]

Several classes of nociceptor are known to produce heat dependent signals associated with threshold for thermal pain (~40 °C−45 °C) and beyond.[10,11] Heat-responsive fibers typically respond to both noxious mechanical and heat stimuli, and include both relatively slow and thin unmyelinated axons called C-fibers, and relatively fast, myelinated A-fibers of both type I and type II.[10] The type II A-fibers in hairy skin send signals at temperatures just below the thermal pain threshold, and are possible mediators of the initial sensations of thermal

Special Issue: Multiscale Biological Materials and Systems: Integration of Experiment, Modeling, and Theory

Received: December 17, 2016
Accepted: February 14, 2017
Published: February 14, 2017

DOI: 10.1021/acsbiomaterials.6b00789
ACS Biomater. Sci. Eng. XXXX, XXX, XXX−XXX

pain in humans via the activation of a member of the transient receptor potential (TRP) cation channel family, TRPV1. Slower developing pain involves C-fibers and other A-fibers.[10,11] C-fibers require longer noxious temperature exposure to reach peak firing rates and involve heat sensors other than TRPV1 channels. Such channels might include TRPV3, TRPV4, and constitutively active K^+ (KCNK2) channels, the latter of which are inhibited by noxious heat.[12,13] A-MH type I fibers might rely upon TRPV2 channels, activated by temperatures greater than 52 °C.

The focus in this article is members of the TRP family, which includes many ion channels involved specifically in thermally evoked pain sensations,[7] particularly in high-threshold nociceptors.[8] Almost all thermally gated ion channels belong to the TRP family, termed as thermo-TRP ion channels.[12,14] Understanding the kinetics temperature-sensitive responses of thermo-TRP ion channels is key to understanding thermal pain sensation.

Although the detailed molecular mechanism underlying the opening of these channels is still a subject of debate, accumulating evidence shows that thermo-TRP ion channels are gated by a shift in temperature at a nociceptor, and thereby provide a basis for temperature sensation.[12,15] This temperature sensing property is closely related to the voltage-dependent gating properties of thermo-TRP channels: changes in temperature induce shifts in the voltage-dependent activation of thermo-TRP channels.[16] The activation of the thermo-TRP channels is well established, with a high likelihood of opening for TRPV1 channels above the thermal pain threshold of 43 °C.[15] However, with prolonged exposure, nociceptors become insensitive to noxious stimuli.[17] Although some decreased sensitivity may revert after noxious stimuli are removed,[18,19] some result from irreversible changes to nociceptors.[20] The underlying gating mechanisms have remained elusive. Experimental characterization and mathematical models of these irreversible changes are needed to advance our understanding of the molecular basis of nociceptor signaling.

Several mathematical models have been developed at the molecular, cellular and neuron network levels that respond well to noxious heating.[9,21−25] Besides, the models that addressed the relationship between the protein conformational changes and the ion channels responses have also been proposed.[26,27] In addition, two-state model[16,28] and the allosteric model[29−31] have also been developed to model the gating behaviors of ion channels. However, these existing models have not considered gate control of ion channels when irreversible thermal desensitization occurs.

Here, we developed a predictive mathematical model that incorporates irreversible thermal desensitization of ion channels and its role in nociceptor transduction mechanisms. The model presented in this paper is a new three-state model for nociceptor transduction coupled with irreversible thermal desensitization of ion channels. The proposed model describes the discharge rate of a nociceptor subjected to different temperatures, including temperatures adequate for thermal desensitization of ion channels. We evaluated the model by comparing simulated results with experimental observations. Both the experimental characterization and mathematical models are expected to advance fundamental understanding of the function of ion channels and to design thermal ablation treatments that can be performed with reduced anesthesia.

2. MATERIALS AND METHODS

2.1. General Approaches. We developed a model to predict nociceptor activation as a function of heating applied to a tissue, and the loss of this activation due to irreversible desensitization of thermo-TRP channels. The model was tested against experiments conducted in vivo in an adult feline model, in which frequency responses were recorded from functional single fibers of the inferior dental nerve while the crown of a lower canine tooth was heated. The model has three levels. First, continuum-level models were used to estimate the temperature fields surrounding an intradental nociceptor. Second, a cellular-level modified Hodgkin-Huxley model was used to predict nociceptor electrophysiology from ionic currents. Third, a new thermo-TRP ion channel model was proposed to estimate the probability of ion channel opening as a function of temperature. The in vivo animal study is illustrated in Figure 1. Details of animal experiment can be found in Supporting Information.

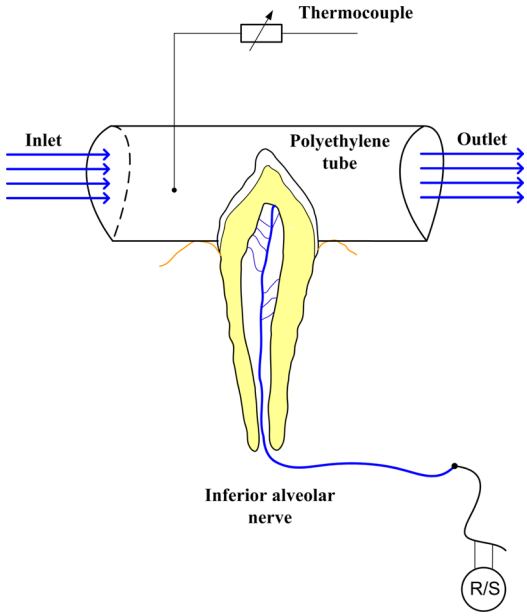

Figure 1. Feline canine tooth were embedded in a specially molded polyethylene tube and heated with isotonic saline at prescribed temperatures. Nociceptive action potentials were recorded as temperature was varied to determine the relationship between saline temperature and the frequency of the spike train observed in the neural discharge data.

2.2. Estimation of Temperature Fields Surrounding Nociceptors. A feline lower canine tooth was modeled to predict the temperature field surrounding a nociceptor during heating of the crown (Figure 2a). We applied finite element method (FEM) using a two-dimensional, axisymmetric tooth model (Figure 2b), which has been demonstrated to provide a good approximation to experimentally observed temperature increases under thermal loading.[32] Initially, the tooth had a constant temperature of 35.2 °C, equal to oral cavity temperature.[33] The tooth crown (boundary ABC, Figure 2c) was subjected to hot sailine stimulation with heat transfer coefficient h = 500 W m^{-2} K^{-1}.[34] The remainder of the exterior tooth surface (boundary CDEF, Figure 2c) lays below the cementoenamel junction (i.e., was embedded in the gum) with a constant temperature of 35.2 °C.[32,35] The boundary AF was thermally insulated, because of the axisymmetric boundary condition. We modeled heat transport in the pulp as being dominated by conduction only, motivated by previous FEM simulations of intradental temperature fields[36] that were confirmed by in vitro experiments.[32] Physical properties of pulp were taken as identical to water, with thermal conductivity k = 0.63 W m^{-1} K^{-1}, mass density $\rho = 1.00 \times 10^3$ kg m^{-3}, and specific heat $c_p = 4.2 \times 10^3$ J kg^{-1} K^{-1}.[34] Physical properties of enamel were thermal

DOI: 10.1021/acsbiomaterials.6b00789
ACS Biomater. Sci. Eng. XXXX, XXX, XXX−XXX

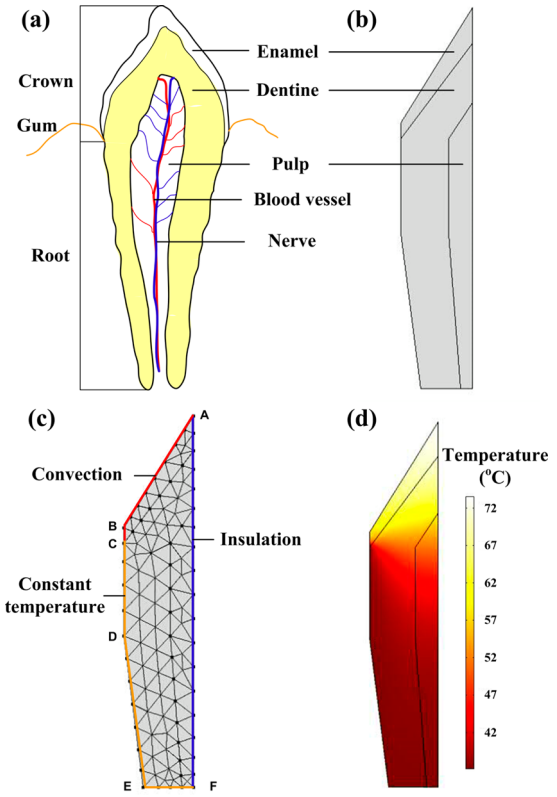

Figure 2. (a) Schematic of the composite structures of a feline canine tooth. (b) Schematic of the 2D three-layer axisymmetric idealization studied. (c) Finite element discretization and schematic of boundary conditions. (d) Representative simulated temperature field for a saline bath temperature of 70 °C.

conductivity 0.81 W m^{-1} K^{-1},[37] mass density 2.80 × 10^3 kg m^{-3}, and specific heat 0.71 × 10^3 J kg^{-1} K^{-1},[38] and those of dentine were thermal conductivity 0.48 W m^{-1} K^{-1},[37] mass density 1.96 × 10^3 kg m^{-3} and specific heat 1.59 × 10^3 J kg^{-1} K^{-1}.[38]

The steady state heat transfer equation was employed to model the temperature field $T(r,z)$ at the pulp horn, where most intrapulpal nerve fibers are located:

$$\nabla^2 T(r, z) = 0 \tag{1}$$

where r and z are axisymmetric space variables.

Equation 1 was solved over the mesh shown in Figure 2c using the commercial FEM package COMSOL 3.3a (COMSOL, Inc., Burlington, MA). The convergence of the simulated temperature fields was checked by mesh refinement tests. Convergence to within a few percent was achieved for a mesh containing 162 triangles elements and 237 nodes.

2.3. Modeling of Nociceptive Signal Transduction. A modified Hodgkin-Huxley model was applied to model the roles of multiple K^+ channels (Figure S1) in the frequency modulation of nociceptors:[23]

$$C_{men}\frac{dV_{men}}{dt} = I_{Na} + I_K + I_L + I_{K2} + I_{st} \tag{2}$$

where V_{mem} is the membrane potential (mV), positive when the membrane is depolarized and negative when the membrane is hyperpolarized; t (ms) is the neuron discharge time; C_{mem} (μF/cm^2) is the membrane capacitance per unit area; I_{Na}, I_K, and I_L are the Na^+, K^+ and transmembrane leakage currents (μA/cm^2), respectively; and I_{K2} is the fast transient K^+ current.[39] The transmembrane currents are determined by the electrical potential difference and the conductance of membrane,[40] so that I_{Na}, I_K, I_L[23,39] and I_{K2}[22] are given by

$$I_{Na} = g_{Na} m^3 h (V_{Na} - V_{men}) \tag{3a}$$

$$I_K = g_K n^4 (V_K - V_{men}) \tag{3b}$$

$$I_L = g_L (V_L - V_{men}) \tag{3c}$$

$$I_{K2} = g_A A^3 B (V_{K2} - V_{men}) \tag{3d}$$

where V_{Na}, V_K, V_L, and V_{K2} are the reversal potentials for the Na^+, K^+, leakage, and fast transient K^+ currents (all in mV), respectively; and g_{Na}, g_K, g_L, and g_A are the maximum ionic conductances of Na^+, K^+, leakage and the fast transient K^+ currents (all in mS/cm^2), respectively. m, h, and n are gating variables; A and B are factors having the same functional significance as factors m and h. Details on the determination of these variables and factors can be found in the Supporting Information.

This modified Hodgkin–Huxley model was used to model the frequency modulation of intradental nociceptors. Given the parallel distribution of ion channels in the membranes of nociceptors, the total stimulation-induced current, I_{st} (μA/cm^2), may be calculated as[22]

$$I_{st} = I_{mech} + I_{heat} + I_{chem} \tag{4}$$

where I_{mech}, I_{heat}, and I_{chem} are separately the transmembrane currents generated by opening the mechanically-, thermally- and chemically gated ion channels (all in μA/cm^2). In this study, only thermal stimulation was applied, therefore, only thermally gated ion channels were considered or the generation of stimulation-induced transmembrane current, so that

$$I_{st} = I_{heat} \tag{5}$$

The quantitative relationship between the stimulation and current can thence be described as[23]

$$I_{heat} = \left(\left[C_{h1}\exp\left(\frac{(T - T_{thr})/T_{thr}}{C_{h2}}\right) + C_{h3}\right] + I_{shift}\right)H(T - T_{thr}) \tag{6}$$

where T_{thr} is the thermal pain threshold temperature; C_{h1}, C_{h2} and C_{h3} are constants; and I_{shift} (μA/cm^2) is the shift current. I_{shift} is determined as described in the Supporting Information. The constants C_{h1} and C_{h3} are set to be 2.0 μA/cm^2 and −1.0 μA/cm^2, respectively, and the dimensionless fitting parameter C_{h2} was set at 2.0. Here, $H(x)$ is the Heaviside function accounting for the threshold process. We note that a spectrum of thermo-TRP channels become activated at temperatures within the noxious range, but focus for simplicity on a single family of channels. As described below, this is justified because the desensitization temperatures of the channels can be expected to be similar.

To model the observation that thermo-TRP channels reach saturation at ∼55 °C,[41] eq 6 was modified as follows to predict the thermal current over a wide temperature range

$$I_{heat} = \begin{cases} \left(C_{h1}\exp\left(\dfrac{T - T_{thr}}{C_{h2}T_{thr}}\right) + C_{h3} + I_{shift}\right)H(T - T_{thr}) \\ \quad (T < 55°C) \\ \left(C_{h1}\exp\left(\dfrac{55 - T_{thr}}{C_{h2}T_{thr}}\right) + C_{h3} + I_{shift}\right)H(55 - T_{thr}) \\ \quad (T > 55°C) \end{cases} \tag{7}$$

2.4. Opening Probability of Thermo-TRP Channels. The dependence of transmembrane current on temperature has been observed experimentally.[9] While the conductance of heat-activated channels is only weakly temperature-dependent,[42] the dependence of transmembrane current on temperature can be attributed to a strong temperature dependence of the probability of channel opening.[9,41] Because thermal gating is controlled by conformational changes to channel proteins,[14,43,44] we hypothesized that the responses of channel

DOI: 10.1021/acsbiomaterials.6b00789
ACS Biomater. Sci. Eng. XXXX, XXX, XXX−XXX

proteins to temperature change (e.g., opening, closing, irreversible desensitization) could be predicted using models similar to temperature-dependent catalytic activity of enzymes. We therefore propose that when the temperature rises above the threshold of 43 °C, inactive TRPV1 ion channels (inactive, closed state, E_{in}) transit reversibly to active channels (active, open state, E_{act}) which subsequently undergo thermal inactivation to the irreversible desensitization state, X:

$$E_{in} \overset{\text{reversible}}{\longleftrightarrow} E_{act} \overset{\text{irrevserible}}{\longrightarrow} X \tag{8}$$

Because irreversible thermal desensitization causes open-state ion channels to undergo irreversible inactivation to a state that does not permit passage of ions, we re-express I_{st} as

$$I_{st} = \lambda I_{heat} \tag{9}$$

where λ is defined as the activity coefficient of the ion channel. λ is governed by the fraction of ion channels available for activity:

$$\lambda = \frac{[E_{in}] + [E_{act}]}{[E_0]} \tag{10}$$

where $[E_{in}]$ denotes the areal concentration (number per unit area) of the closed state ion channels; $[E_{act}]$ denotes the areal concentration of open state ion channels; and $[E_0]$ represents the areal concentration of ion channels that would be available in the absence of irreversible desensitization. Since the heat induced irreversible desensitization process in our case is relatively short compared to the process of ion channel synthesis, areal concentrations can be approximately assumed to be conserved

$$[E_0] = [E_{inact}] + [E_{act}] + [X] \tag{11}$$

A mass balance for the ion channel leads to

$$[E_{act}] = \frac{[E_0] - [X]}{1 + K_{eq}} \tag{12}$$

where $[X]$ is concentration of irreversibly desensitized ion channel and K_{eq} denotes the equilibrium constant for the reversible step ($E_{in} \overset{\text{reversible}}{\longleftrightarrow} E_{act}$). K_{eq} obeys the van't Hoff equation[45]

$$K_{eq} = e^{\Delta H_{eq}/R(1/T_m 1/T)} \tag{13}$$

where ΔH_{eq} = 150 kcal/mol represents the enthalpy change associated with the conversion of an ion channel from the open to closed state;[41] T_m = 320 K was the midpoint of the transition between the open and closed states of the population of ion channels; R = 8.314 J/(mol K) is the universal gas constant.

Following kinetics similar to denaturation of enzymes, the irreversible heat-induced desensitization of thermo-TRP channels ($E_{act} \overset{\text{irreversible}}{\longrightarrow} X$) follows:[46]

$$[X] = [E_0]\left(1 - \frac{1}{D_0}\frac{(1 + K_{eq})^2}{K_{eq}^2 k_{inact}[E_0]t}\right)^{-1} \tag{14}$$

where the diffusion constant D_0 = 1 m^2/s is an arbitrary fitting parameter. The variation of the thermal denaturation rate constant k_{inact} with temperature is given by

$$k_{inact} = \frac{k_B T}{h} e^{-\Delta G_{inact}/RT} \tag{15}$$

Where ΔG_{inact} = 95 kJ/mol denotes activation energy for thermal denaturation; k_B = 1.381 × 10^{-26} kJ/K is Boltzmann's constant; h = 6.626 × 10^{-37} kJ s is Planck's constant. Equations 10−15 could be solved to obtain the activity coefficient λ as a function of time at a given temperature. The parameters used in the paper are listed in Table 1.

Table 1. Parameters Used

parameters	value	ref
heat transfer coefficient	h = 500 W m^{2-} K^{-1}	31
thermal conductivity	k = 0.63 W m^{-1} K^{-1}	31
mass density	ρ = 1.00 × 10^3 kg m^{-3}	31
specific heat	c_p= 4.2 × 10^3 J kg^{-1} K^{-1}	31
thermal conductivity (enamel)	0.81 W m^{-1} K^{-1}	34
mass density (enamel)	2.80 × 10^3 kg m^{-3}	35
specific heat (enamel)	0.71 × 10^3 J kg^{-1} K^{-1}	35
thermal conductivity (dentine)	0.48 W m^{-1} K^{-1}	34
mass density (dentine)	1.96 × 10^3 kg m^{-3}	35
specific heat (dentine)	1.59 × 10^3 J kg^{-1} K^{-1}	35
C_{h1}	2.0 μA/cm^2	
C_{h2}	2.0 (dimensionless)	
C_{h3}	−1.0 μA/cm^2	
saturation of thermo-TRP channels	∼55 °C	38
enthalpy change associated with the conversion of an ion channel	ΔH_{eq} = 150 kcal/mol	38
midpoint of the transition between the open and closed states of the population of ion channels	T_m = 320 K	
universal gas constant	R = 8.314 J/(mol K)	
activation energy for thermal denaturation	ΔG_{inact} = 95 kJ/mol	
Boltzmann's constant	K_B = 1.381 × 10^{-26}kJ/K	
Planck's constant	h = 6.626 × 10^{-37} kJ s	

3. RESULTS AND DISCUSSION

Slow heating of the canine tooth crown elevated the temperature of the pulp, especially in the nominally conical "pulp horn" that extends toward the crown. A FEM simulation of this steady state elevation in temperature (Figure 2d) showed a spatial gradient from the crown surface, where the greatest temperature rise occurred, to the portions of the tooth nearest the gum, where the lowest temperature rise occurred. Throughout the interior of the tooth, the temperature increased with increasing saline temperature applied to the crown. Of primary interest to the pain response is the temperature of the tissue within the pulpal horn, because this region is heavily innervated by intra pulpal nerve fibers.[47] Therefore, temperatures from this region were used to model the nociceptive transduction. The average temperature over this region scaled almost linearly with the saline temperature over the range of testing conditions (Figure 3).

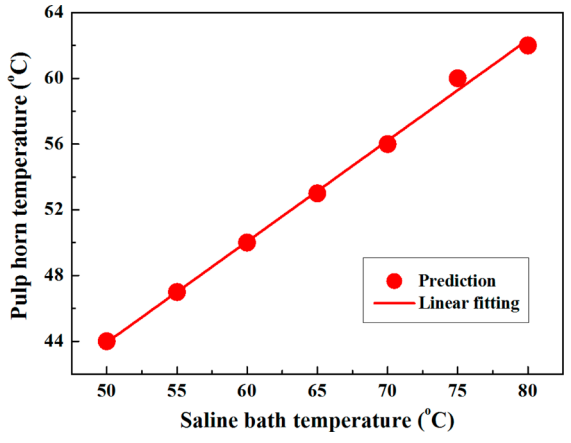

Figure 3. Over the range studied, the steady rise in mean temperature over the pulp horn was nearly linear with the rise in the temperature of the saline bath.

DOI: 10.1021/acsbiomaterials.6b00789
ACS Biomater. Sci. Eng. XXXX, XXX, XXX−XXX

Tooth pain sensations involve activation of mechanosensitive or thermosensitive nociceptors in tooth pulpal afferents.[48,49] Mechanosensitive nociceptors that can be activated by dentinal fluid flow can contributed to tooth pain sensations.[50−52] Elevation of temperature near the pulp horn can excite the dense population of thermosensitive nociceptors (thermo-TRP) in that region, generating a series of periodic voltage spikes whose frequency can also be transduced as pain.[46] In our experiments, these nociceptor discharges came at a frequency of approximately 3 Hz for saline bath temperatures of 50−55 °C, and then increased gradually to approximately 30 Hz at saline bath temperature of 70 °C (corresponding to temperature of ∼56 °C around ion channels), presumably as TRPV1 channels reached saturation, and as TRPV2 channels opened (Figure 4,

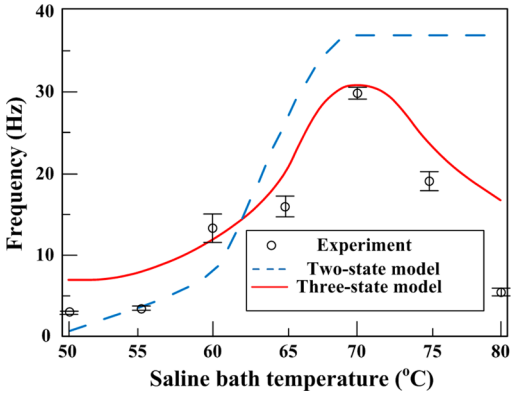

Figure 4. Experimental measurement of discharge frequency in a heated feline canine tooth showed a rise in frequency associate with saline bath temperature of 70 °C, but a reduction thereafter. The state-of-the-art two-state model incorrectly predicts a sustained, high frequency response at all temperatures above this. The new three-state model correctly predicts a reduction in nociceptor discharge frequency for saline bath temperatures above 70 °C. Plotted is the predicted state after 5 min of thermal stimulation.

circular symbols). Note that Figure 4 represents the state after 5 min of thermal stimulation. For heating at even higher temperature, the discharge frequency reduced gradually to approximately 5 Hz at 80 °C.

To model these responses from the estimates of pulp horn temperatures, we applied a modified Hodgkin−Huxley model for nociceptor action potential, and models for opening of thermo-TRP ion channels at the distal ends of these nociceptors. The model for the latter is the two-state model, in which all thermo-TRP channels oscillate between open and closed states, with the probability of opening becoming much larger beyond a critical temperature. While this model predicts a rise in nociceptor discharge frequency at low temperatures, it cannot capture the loss of thermo-TRP channel functionality and associated reduction in nociceptor discharge frequency at high temperatures (Figure 4, dashed line). With the two-state model, the probability of opening for thermo-TRP channels stays high as a constant at high temperatures, resulting in the constant discharge frequency, no matter how high the temperature is. This prediction is not supported by our experimental data.

We hypothesized that the loss of functionality of the thermo-TRP channels could be modeled with existing models for temperature-induced loss of enzymatic function, and therefore proposed a three-state model. The three-state model extended the two-state model by adding a transition to a new irreversible closed state, beyond a critical temperature. In this model, thermo-TRP channels transit from an inactive state (low opening probability) to an active state (high opening probability) when heated and subsequently to an irreversible desensitization state. The influence of irreversible desensitization on availability of ion channels is quantified by the activity coefficient, λ (Figure 5, solid curve, representing the state after

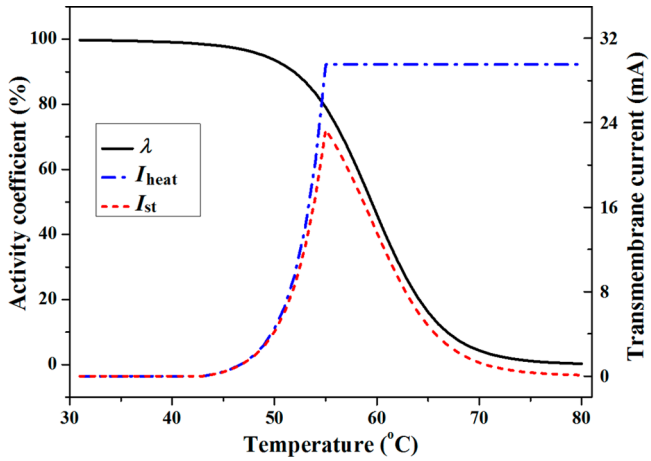

Figure 5. For the two-state model, the transmembrane current I_{heat} rises to a steady state value that is sustained for all nociceptor temperatures above 55 °C. However, when considering the irreversible thermal denaturation of thermo-TRP channels, we note that the activity coefficient, λ, drops with increasing temperature, reducing the availability of thermo-TRP channels. The new three-state model involves a transmembrane current I_{st} that is scaled down from I_{heat} by this factor, λ, and that therefore drops beyond a critical temperature. Plotted is the predicted state after 5 min of thermal stimulation.

5 min of thermal stimulation.). At low temperatures, the activity coefficient was nearly unity, meaning that low temperatures would not reduce the availability of thermo-TRP channels. However, the activity coefficient decreased with increasing temperature, with the sharpest drop in the range of 45−70 °C over which the activity coefficient decreased from 98 to 4.3%. This sharp decrease suggests that at high temperatures, a majority of ion channels lose function due to irreversible desensitization of these ion channels.

The result of this desensitization is a reduction of the transmembrane current associated with thermo-TRP channels at high temperatures. In the absence of irreversible desensitization, as is the case in the two-state model, the thermo-TRP channels transit from the closed to the open state. This contributes to an increase in transmembrane current with increasing temperature (Figure 5, dashed-dot curve). For the two-state model, the transmembrane current increased exponentially from zero at 43 °C (temperature surrounding nociceptors) to a peak of 29.5 mA at 55 °C. Thereafter, transmembrane currents were predicted to be sustained at this peak level for all temperatures above 55 °C. However, this behavior is not consistent with experiment or with the observation that channel protein structures become unstable and lose function at sufficiently high temperature. This motivated the development of the proposed three-state model, in which open state ion channels can undergo a potentially irreversible desensitization at elevated temperatures. This shift from the open state to a irreversibly desensitized state

DOI: 10.1021/acsbiomaterials.6b00789
ACS Biomater. Sci. Eng. XXXX, XXX, XXX−XXX

reduced the transmembrane current by reducing the total number of available ion channels, as represented by the drop in activity coefficient with increasing temperature. The prediction of temperature-stimulated transmembrane current (Figure 5, dashed curve) is the product of the transmembrane current that would exist in the absence of irreversible desensitization (Figure 5, dashed-dot curve) and the activity coefficient (Figure 5, solid curve). This current reaches a peak of 23.3 mA at ∼55 °C and then decreases with further increase in temperature.

The reduction in transmembrane current as induced by irreversible desensitization results in a reduction of nociceptor discharge frequency similar to that observed experimentally (Figure 4, solid curve), with a peak at approximately 70 °C (saline temperature) followed by a steady decrease. This supports our hypothesis and shows that, at the very least, the reductions in nociceptor discharge frequency at high temperature as we observed experimentally are consistent with the kinetics of denaturation of catalytic enzymes.

A few limitations of the three-state model need to be emphasized. First, the three-state model considered only a single class of thermo-TRP channels, specifically the TRPV1 channels. A second class, the TRPV2 channels, become activated over the temperature range of our experiments, and their effects might be evident in the rise of nociceptor discharge frequency observed at a saline bath temperature of 60 °C. However, we opted against the inclusion of two separate thermo-TRP channel classes in this first study because including a second would introduce additional unknowns associated with the other two limitations we will mention, namely the specificity of the model, and the number of free parameters.

Concerning the specificity of the three-state model, the kinetics of thermo-TRP channel irreversible desensitization were based upon published values for enzymatic denaturation, rather than upon first principles simulation of the effect of temperature on thermo-TRP channel function. As the latter becomes available, it would be desirable to repeat the current study with numerically derived rather than modeling of activity coefficient. However, a simplified and somewhat generic model served here to show that the irreversible desensitization of a single class of thermo-TRP channels is adequate for replicating experimental observation.

Both the two-state model and the developed three-state model have a number of coefficients need to be determined by fitting to experimental data. That is why the two models do not converge for lower temperatures. These could be fitted as well through first principles simulations, and the current study should be revisited when these data become available.

Despite these limitations, results of this study suggest that the irreversible desensitization of thermo-TRP channel is a possible source of the reduction in nociceptor discharge frequency at very high temperatures. Although the presented model is just an oversimplification, it provides the first foundation for the design of thermal ablation and dental drilling procedures that have as an end point for the elimination of pain by thermo-TRP desensitization. As these models become more refined, the possibility of thermal treatments for pain abatement and design of anesthesia-free thermal ablation therapies will be brought closer to reality.

4. CONCLUSION

In conclusion, we developed a three-state model to simulate the dynamic response of thermo-TRP channels to a range of temperatures, and applied this to predict discharge frequencies measured in vivo from heated dental tissue. Although the three-state model simplifies the dynamic temperature responses of thermo-TRP channels, it is capable of capturing the essence of the experimental observations, supporting the principle of irreversible thermal desensitization of thermo-TRP channels underlying the loss of sensation at high temperature.

■ ASSOCIATED CONTENT

Supporting Information

The Supporting Information is available free of charge on the ACS Publications website at DOI: 10.1021/acsbiomaterials.6b00789.

Ethics statement, animal tests, determination of variables associated with H−H model, shift current, and Schematic of the original and modified Hodgkin-Huxley model (PDF)

■ AUTHOR INFORMATION

Corresponding Authors

*E-mail: minlin@mail.xjtu.edu.cn.
*E-mail: fengxu@mail.xjtu.edu.cn.

ORCID

Min Lin: 0000-0002-3259-1955
Feng Xu: 0000-0003-4351-0222

Notes

The authors declare no competing financial interest.

■ ACKNOWLEDGMENTS

This work was financially supported by the National Natural Science Foundation of China (11402192), Fundamental Research Funds for the Central Universities (2016qngz03, 2015qngz09), Opening Project of Key Laboratory of Shaanxi Province for Craniofacial Precision Medicine Research, College of Stomatology, Xi'an Jiaotong University (2016LHM-KFKT007), the Chinese Ministry of Education through a Changjiang Scholar Award to G.M.G, and the U.S. National Science Foundation Center for Engineering Mechanobiology, Grant CMMI 1548571.

■ REFERENCES

(1) Hubbard, R. D.; Chen, Z.; Winkelstein, B. A. Transient cervical nerve root compression modulates pain: Load thresholds for allodynia and sustained changes in spinal neuropeptide expression. *J. Biomech.* **2008**, *41*, 677−685.

(2) Besier, T. F.; Fredericson, M.; Gold, G. E.; Beaupré, G. S.; Delp, S. L. Knee muscle forces during walking and running in patellofemoral pain patients and pain-free controls. *J. Biomech.* **2009**, *42*, 898−905.

(3) Baisi, A.; De Simone, M.; Raveglia, F.; Cioffi, U. Thermal ablation in the treatment of lung cancer: Present and future. *Eur. J. Cardiothorac. Surg.* **2013**, *43*, 683−686.

(4) Reader, A.; Nusstein, J. Local anesthesia for endodontic pain. *Endodontic Topics* **2002**, *3*, 14−30.

(5) Nixdorf, D. R.; Moana-Filho, E. J.; Law, A. S.; McGuire, L. A.; Hodges, J. S.; John, M. T. Frequency of persistent tooth pain after root canal therapy: A systematic review and meta-analysis. *J. Endod.* **2010**, *36*, 224−230.

(6) McCleskey, E. W.; Gold, M. S. Ion channels of nociception. *Annu. Rev. Physiol.* **1999**, *61*, 835−856.

(7) Venkatachalam, K.; Montell, C. Trp channels. *Annu. Rev. Biochem.* **2007**, *76*, 387−417.

(8) Wang, H.; Woolf, C. J. Pain TRPs. *Neuron* **2005**, *46*, 9−12.

DOI: 10.1021/acsbiomaterials.6b00789
ACS Biomater. Sci. Eng. XXXX, XXX, XXX−XXX

(9) Cesare, P.; Moriondo, A.; Vellani, V.; McNaughton, P. A. Ion channels gated by heat. *Proc. Natl. Acad. Sci. U. S. A.* **1999**, *96*, 7658−7663.
(10) Dubin, A. E.; Patapoutian, A. Nociceptors: the sensors of the pain pathway. *J. Clin. Invest.* **2010**, *120*, 3760−3772.
(11) Raja, S. N.; Meyer, R. A.; Campbell, J. N. Peripheral mechanisms of somatic pain. *Anesthesiology* **1988**, *68*, 571−590.
(12) Patapoutian, A.; Peier, A. M.; Story, G. M.; Viswanath, V. ThermoTRP channels and beyond: Mechanisms of temperature sensation. *Nat. Rev. Neurosci.* **2003**, *4*, 529−539.
(13) Alloui, A.; Zimmermann, K.; Mamet, J.; et al. TREK-1, a K+ channel involved in polymodal pain perception. *EMBO J.* **2006**, *25*, 2368−2376.
(14) Ramsey, I. S.; Delling, M.; Clapham, D. E. An introduction to TRP channels. *Annu. Rev. Physiol.* **2006**, *68*, 619−647.
(15) Woolf, C. J.; Ma, Q. Nociceptors–noxious stimulus detectors. *Neuron* **2007**, *55*, 353−364.
(16) Voets, T.; Droogmans, G.; Wissenbach, U.; Janssens, A.; Flockerzi, V.; Nilius, B. The principle of temperature-dependent gating in cold- and heat-sensitive TRP channels. *Nature* **2004**, *430*, 748−754.
(17) Caterina, M. J.; Schumacher, M. A.; Tominaga, M.; Rosen, T. A.; Levine, J. D.; Julius, D. The capsaicin receptor: A heat-activated ion channel in the pain pathway. *Nature* **1997**, *389*, 816−824.
(18) Treede, R.-D.; Meyer, R. A.; Campbell, J. N. Myelinated mechanically insensitive afferents from monkey hairy skin: Heat-response properties. *J. Neurophysiol.* **1998**, *80*, 1082−1093.
(19) Peng, Y. B.; Ringkamp, M.; Meyer, R. A.; Campbell, J. N. Fatigue and paradoxical enhancement of heat response in c-fiber nociceptors from cross-modal excitation. *J. Neurosci.* **2003**, *23*, 4766−4774.
(20) Jancso, G.; Kiraly, E.; Jancso-Gabor, A. Pharmacologically induced selective degeneration of chemosensitive primary sensory neurons. *Nature* **1977**, *270*, 741−743.
(21) Nadkarni, S.; Jung, P. Spontaneous oscillations of dressed neurons: A new mechanism for epilepsy? *Phys. Rev. Lett.* **2003**, *91*, 268101.
(22) Hodgkin, A. L.; Huxley, A. F. A quantitative description of membrane current and its application to conduction and excitation in nerve. *J. Physiol.* **1952**, *117*, 500−544.
(23) Xu, F.; Wen, T.; Lu, T. J.; Seffen, K. A. Modeling of nociceptor transduction in skin thermal pain sensation. *J. Biomech. Eng.* **2008**, *130*, 041013−041013.
(24) Xu, F.; Lu, T. J.; Seffen, K. A. Skin thermal pain modeling—a holistic method. *J. Therm. Biol.* **2008**, *33*, 223−237.
(25) Xu, F.; Lin, M.; Lu, T. J. Modeling skin thermal pain sensation: Role of non-fourier thermal behavior in transduction process of nociceptor. *Comput. Biol. Med.* **2010**, *40*, 478−486.
(26) Chung, S. H.; Corry, B. Three computational methods for studying permeation, selectivity and dynamics in biological ion channels. *Soft Matter* **2005**, *1*, 417−427.
(27) Cantor, R. S.; Twyman, K. S.; Milutinovic, P. S.; Haseneder, R. A kinetic model of ion channel electrophysiology: Bilayer-mediated effects of agonists and anesthetics on protein conformational transitions. *Soft Matter* **2009**, *5*, 3266−3278.
(28) Voets, T.; Nilius, B. Quantifying and modeling the temperature-dependent gating of trp channels. *Rev. Physiol., Biochem. and Pharmacol.* **2012**, *162*, 91−119, DOI: 10.1007/112_2011_5.
(29) Brauchi, S.; Orio, P.; Latorre, R. Clues to understanding cold sensation: Thermodynamics and electrophysiological analysis of the cold receptor TRPM8. *Proc. Natl. Acad. Sci. U. S. A.* **2004**, *101*, 15494−15499.
(30) Yao, J.; Liu, B.; Qin, F. Kinetic and energetic analysis of thermally activated TRPV1 channels. *Biophys. J.* **2010**, *99*, 1743−1753.
(31) Jara-Oseguera, A.; Islas León, D. The role of allosteric coupling on thermal activation of thermo-TRP channels. *Biophys. J.* **2013**, *104*, 2160−2169.
(32) Jakubinek, M. B.; O'Neill, C.; Felix, C.; Price, R. B.; White, M. A. Temperature excursions at the pulp-dentin junction during the curing of light-activated dental restorations. *Dent. Mater.* **2008**, *24*, 1468−1476.
(33) Tunc, E. P. Finite element analysis of heat generation from different light-polymerization sources during cementation of all-ceramic crowns. *J. Prosthet. Dent.* **2007**, *97*, 366−374.
(34) Lin, M.; Liu, S. B.; Niu, L.; Xu, F.; Lu, T. J. Analysis of thermal-induced dentinal fluid flow and its implications in dental thermal pain. *Arch. Oral Biol.* **2011**, *56*, 846−854.
(35) Spierings, T. A.; de Vree, J. H.; Peters, M. C.; Plasschaert, A. J. The influence of restorative dental materials on heat transmission in human teeth. *J. Dent. Res.* **1984**, *63*, 1096−1100.
(36) de Vree, J. H.; Spierings, T. A.; Plasschaert, A. J. A simulation model for transient thermal analysis of restored teeth. *J. Dent. Res.* **1983**, *62*, 756−759.
(37) Lin, M.; Liu, Q. D.; Kim, T.; Xu, F.; Bai, B. F.; Lu, T. J. A new method for characterization of thermal properties of human enamel and dentine: Influence of microstructure. *Infrared Phys. Technol.* **2010**, *53*, 457−463.
(38) Brown, W. S.; Dewey, W. A.; Jacobs, H. R. Thermal properties of teeth. *J. Dent. Res.* **1970**, *49*, 752−755.
(39) Lin, M.; Luo, Z. Y.; Bai, B. F.; Xu, F.; Lu, T. J. Fluid mechanics in dentinal microtubules provides mechanistic insights into the difference between hot and cold dental pain. *PLoS One* **2011**, *6*, e18068.
(40) Hodgkin, A. L. *The Conduction of the Nervous Impulses*; Liverpool University Press: Liverpool, U.K., 1964.
(41) Liu, B. Y.; Hui, K. Y.; Qin, F. Thermodynamics of heat activation of single capsaicin ion channels VR1. *Biophys. J.* **2003**, *85*, 2988−3006.
(42) Reichling, D. B.; Levine, J. D. Heat transduction in rat sensory neurons by calcium-dependent activation of a cation channel. *Proc. Natl. Acad. Sci. U. S. A.* **1997**, *94*, 7006−7011.
(43) Lumpkin, E. A.; Caterina, M. J. Mechanisms of sensory transduction in the skin. *Nature* **2007**, *445*, 858−865.
(44) Salazar, H.; Jara-Oseguera, A.; Hernandez-Garcia, E.; Llorente, I.; Arias-Olguin, I. I.; Soriano-Garcia, M.; Islas, L. D.; Rosenbaum, T. Structural determinants of gating in the trpv1 channel. *Nat. Struct. Mol. Biol.* **2009**, *16*, 704−710.
(45) Van Holde, K. E.; Johnson, W. C.; Ho, P. S. *Principles of Physical Biochemistry*; Prentice Hall: Upper Saddle River, NJ, 2006.
(46) Patnaik, P. R. Temperature optima of enzymes: Sifting fact from fiction. *Enzyme Microb. Technol.* **2002**, *31*, 198−200.
(47) Byers, M. R.; Narhi, M. V. O. Dental injury models: Experimental tools for understanding neuroinflammatory interactions and polymodal nociceptor functions. *Crit. Rev. Oral Biol. Med.* **1999**, *10*, 4−39.
(48) Hermanstyne, T. O.; Markowitz, K.; Fan, L.; Gold, M. S. Mechanotransducers in rat pulpal afferents. *J. Dent. Res.* **2008**, *87*, 834−838.
(49) Chung, M.-K.; Lee, J.; Duraes, G.; Ro, J. Y. Lipopolysaccharide-induced pulpitis up-regulates trpv1 in trigeminal ganglia. *J. Dent. Res.* **2011**, *90*, 1103−1107.
(50) Su, K. C.; Chang, C. H.; Chuang, S. F.; Ng, E. Y. K. The effect of dentinal fluid flow during loading in various directions-simulation of fluid−structure interaction. *Arch. Oral Biol.* **2013**, *58*, 575−582.
(51) Su, K. C.; Chuang, S. F.; Ng, E. Y. K.; Chang, C. H. An investigation of dentinal fluid flow in dental pulp during food mastication: Simulation of fluid−structure interaction. *Biomech. Model. Mechanobiol.* **2014**, *13*, 527.
(52) Andrew, D.; Matthews, B. Displacement of the contents of dentinal tubules and sensory transduction in intradental nerves of the cat. *J. Physiol. (Oxford, U. K.)* **2000**, *529*, 791−802.

DOI: 10.1021/acsbiomaterials.6b00789
ACS Biomater. Sci. Eng. XXXX, XXX, XXX−XXX